The Iraqi Journal For Mechanical And Material Engineering, Special Issue (D)

Theoretical Study and Simulation of Corrugated Silicon Diaphragms

Mohammed Midhat Hasan
Department of Mechanical Engineering
College of Engineering
University of Anbar
E-mail: mhmeam@yahoo.com

Abstract

In this paper, silicon diaphragms with planar and corrugated shapes are studied through both theory and simulations. The analytical calculations of deflections are compared with FEM simulations with good agreement. The results show that linear load-deflection relationship can be obtained by increasing corrugation depth and corrugation pitch did not show any noticeable effect compared to other parameters. Therefore the rule of thumb in the design of a corrugated diaphragm is that increasing diaphragm diameter and/or decreasing diaphragm thickness increase diaphragm sensitivity and that increasing corrugation depth increases the linearity of load-deflection relation.

الخلاصة

في هذا البحث، تم دراسة الأغشية المصنوعة من السليكون بأشكالها المستوية والمموجة من خلال النظرية والمحاكاة. قورنت النتائج النظرية للانحرافات مع المحاكاة بواسطة العناصر المحددة وبتوافق جيد. تشير النتائج الى أن العلاقة الخطية للانحراف مع الحمل من الممكن الحصول عليها عن طريق زيادة عمق التموج، وأن خطوة التموج لم تظهر أي تأثير ملحوظ مقارنة مع بقية العوامل. لذا، ففي تصميم الغشاء المموج فان زيادة قطر الغشاء و/أو تقليل سمك الغشاء يزيد من حساسية الغشاء، وأن زيادة عمق التموج يزيد من خطية العلاقة بين الانحراف والحمل.

Introduction

The vast majority of micromachined silicon diaphragms have been flat and either square or rectangular. These configurations have served well for piezoresistive pressure sensors for pressure ranges above about 14 MPa. For very low pressure ranges, however, the non-linearity caused by membrane stresses in a square diaphragm becomes appreciable, and other, more elaborate schemes are needed. These have primarily taken the form of bossed regions on the backside of the diaphragm to concentrate stress at the periphery for piezoresistive devices or to produce piston-like travel from the central region of the diaphragm [1-3] These bossed structures offer better linearity than a non-bossed structure, but the linear deflection possible from such structures is still very small. It has been recognized for decades in the field of conventionally formed metal diaphragms that by introducing corrugations into the diaphragm structure, the linearity of a diaphragm can be increased considerably [4]. To this point it seems that only a limited amount of work has been undertaken to transfer conventional corrugated diaphragm technology to micromachined silicon structures [5]. Micromachining has been demonstrated in a variety of materials including glasses, ceramics, polymers, metals, and various other alloys. But silicon is so strongly associated with MEMS (microelectromechanical systems). The main reasons are given here [6]:

- Its wide use within the microelectronic integrated circuit industry;
- Well understood and controllable electrical properties;
- Availability of existing design tools;
- Economical to produce single crystal substrates;
- Vast knowledge of the material exists;
- Its desirable mechanical properties.

The final point is, of course, particularly desirable for mechanical microsensors. Single crystal silicon is elastic (up to its fracture point), is lighter than aluminum, and has a modulus of elasticity similar to stainless steel. Its mechanical properties are anisotropic and hence are dependent on the orientation to the crystal axis [7]. Table (1) illustrates some of the main properties of silicon in relation to other materials. Stainless steel is used as a convenient reference as it is widely used in the manufacture of traditional mechanical transducers. It must be noted, however, that there are many different types of stainless steel exhibiting a broad variation to those values listed here. Silicon itself exists in three forms: crystalline, amorphous, and polycrystalline (polysilicon). High purity, crystalline silicon substrates are readily available as circular wafers with typical diameters of 100, 150, 200, or 300mm in a variety of thicknesses. Amorphous silicon does not have a regular crystalline form and contains many defects. Its main use has been in solar cells, photo-sensors, and liquid crystal displays. Both amorphous and polysilicon can be deposited as thin-films, usually less than about 5 μm thickness. Other materials that are often used within the MEMS fabrication process include glasses, quartz, ceramics, silicon nitride and carbide, alloys of various metals, and a variety of specialist materials that are used for very specific purposes.

Table (1) Properties of Silicon and Selected Other Materials

Property	*Si {111}*	*Stainless Steel*	*Al*
Young's modulus (GPa)	190	200	70
Poisson's ratio	0.22	0.3	0.33
Density (g/cm^3)	2.3	8	2.7
Yield strength (GPa)	7	3	0.17
Thermal coefficient of expansion (10/^{o}K)	2.3	16	24
Thermal conductivity at 300K (W/cm·^{o}K)	1.48	0.2	2.37

MEMS Simulation and Design Tools

Simulation of micromachined systems and sensors is becoming increasingly important. Before fabricating a prototype, one wishes to virtually build the device and predict its behavior. This allows for the optimization of the various design parameters according to the specifications. As it is a virtual device, parameters can be changed much more quickly than actually fabricating a prototype, then redesigning and fabricating it again. This considerably reduces the time to market and also the cost to develop a commercial device. Any MEMS simulation software uses either System level (or behavioral or reduced order or lumped parameter) modeling, which captures the main characteristics of a MEMS device or finite element modeling (FEM), which originated from mechanical engineering where it was used to predict mechanical responses to a load, such as forces and moments, applied to a part. The part to be simulated is broken down into small, discrete elements—a process called meshing. Each element has a number of nodes and its corners at which it interacts with neighboring elements. The analysis can be extended to non mechanical loads, for example, temperature. Additionally, finite element simulation techniques have been successfully applied to simulate electromagnetic fields, thermodynamic problems such as squeeze film damping, and fluidics. FEM results in more realistic simulation results than behavioral modeling, but it is much more computationally demanding and hence it is difficult to simulate entire systems.

Several example MEMS simulations can be found on the Internet [8, 9]. In the present work, ANSYS structural analysis is used to simulate the corrugated diaphragm's response to applied pressure.

Diaphragm-Based Pressure Sensors

The application of MEMS to the measurement of pressure is a mature application of micromachined silicon mechanical sensors, and devices have been around for more than 35 years. It is without doubt one of the most successful application areas, accounting for a large portion of the MEMS market. Pressure sensors have been developed that use a wide range of sensing techniques, from the most common piezoresistive type to high-performance resonant pressure sensors [10]. The suitability of MEMS to mass-produced miniature high-performance sensors at low cost has opened up a wide range of applications. Examples include automotive manifold air and tire pressure, industrial process control, hydraulic systems, microphones, and intravenous blood pressure measurement. Normally the pressurized medium is a fluid, and pressure can also be used to indirectly determine a range of other measurands such as flow in a pipe, volume of liquid inside a tank, altitude, and air speed.

Diaphragms are the simplest mechanical structure suitable for use as a pressure sensing element. They are used as a sensor element in both traditional and MEMS technology pressure sensors. In the case of MEMS, due to the planar nature of many established fabrication processes, the diaphragm is the main form of sensor element developed. Pressure applied to one (or both) side(s) of the diaphragm will cause it to deflect until the elastic force balances the pressure. The pressure range of a given diaphragm will depend upon its dimensions (surface area and thickness), geometry, edge conditions, and the material from which it is made. Traditional metal diaphragm pressure sensors are made from a range of materials such as stainless steels 316L, 304, 17-4PH, PH 15-7Mo, titanium, nickel alloys, and beryllium copper. The metals are characterized by good elastic properties and media compatibility. In the case of traditional sensors, diaphragms are the simplest sensor element to manufacture, they are the least sensitive to vibrations, they offer the best dynamic response, and they are compatible with simple forms of overload protection. However, the deflection associated with diaphragms is much less than, for example, Bourdon tubes. Therefore, electromechanical transduction mechanisms may be employed to measure the deflection rather than the mechanical linkages associated with Bourdon tubes. Metal diaphragms are typically circular and may incorporate corrugations to modify diaphragm characteristics. The behavior of a diaphragm will depend upon many factors, such as the edge conditions and the deflection range compared to diaphragm thickness. The edge conditions of a diaphragm will depend upon the method of manufacture and the geometry of the surrounding structure. It will vary between a simply supported or rigidly clamped structure. Simply supported diaphragms will not occur in practice, but the analytical results for such a structure may more accurately reflect the behavior of a poorly clamped diaphragm than the rigidly clamped analysis. At small deflections (less than 10% of the diaphragm thickness) the pressure-deflection relationship will be linear. As the pressure increases, the rate of deflection decreases and the pressure-deflection relationship will become nonlinear. As a rule of thumb, a deflection of 12% of diaphragm thickness will produce a terminal nonlinearity of 0.2%; a deflection of 30% produces a nonlinearity of 2% [11]. The suitability of the deflection range will depend upon the desired specification of the sensor and the acceptable degree of compensation. Very thin diaphragms with large deflection can be considered as membranes. In theory, a membrane has no flexural rigidity and experiences tensile stress, but no bending stress. A flat diaphragm with a thicker center portion named bossed diaphragm, which increases the rigidity in that location. The inclusion of the center section, or boss, affects the behavior of the diaphragm under pressure. A bossed diaphragm, for example, will exhibit higher stresses for a given deflection, which is attractive in the case of a traditional bonded strain gauge pressure sensor. They are particularly well suited to sensing low pressures and exhibit improved linearity characteristics compared with flat diaphragms. The boss should be a minimum of six times thicker than the diaphragm and the ratio of boss radius to diaphragm radius should be greater than 0.15 for the boss to be effective [11].

Flat Diaphragms

The deflection of a flat, clamped, circular diaphragm under a pressure difference is given approximately by [11]:

$$\frac{PR^4}{Eh^4} = \frac{5.33}{1-\nu^2}\left(\frac{y}{h}\right) + \frac{2.38}{1-\nu^2}\left(\frac{y^3}{h^3}\right)$$

where P is the pressure difference across the diaphragm, R is the diaphragm radius, h is the diaphragm thickness, E is Young's modulus, ν is Poisson's ratio and y is the center deflection of the diaphragm.
This equation assumes the following assumptions:

- The diaphragm is flat and of uniform thickness.
- The material is homogenous and isotropic.
- Pressure is applied normally to the plane of the diaphragm.
- The elastic limit of the material is not exceeded.
- The thickness of the diaphragm is not too thick (maximum 20% of diaphragm diameter).
- Deformation is due to bending, the neutral axis of the diaphragm experiences no stress.

For comparison purposes, the equivalent square diaphragm deflection is given by [12]:

$$\frac{Pa^4}{Eh^4} = \frac{4.2}{1-\nu^2}\left(\frac{y}{h}\right) + \frac{1.58}{1-\nu^2}\left(\frac{y^3}{h^3}\right)$$

where a is the half sidelength. Thus a circular diaphragm with a radius equal to the half sidelength of a square diaphragm will be about 30% stiffer, for small deflections, and the nonlinearity will be very similar, due to the nearly equal ratios of linear to cubic coefficients. Note that in either case the nonlinearity becomes significant for deflections more than about 25% of the thickness of the diaphragm, regardless of the radius of the diaphragm. This is of great importance in the design of very sensitive micromachined diaphragms, particularly for capacitive sensing applications.

Corrugated Diaphragms

With the introduction of corrugations into the diaphragm structure the situation can be changed dramatically. Corrugations in a diaphragm enable operation at larger displacements with improved linearity. The corrugations can have sinusoidal, triangular, rectangular, trapezoidal, and toroidal profiles. While this has a small influence on the behavior of the diaphragm, the depth of corrugation and material thickness are the main factors [see figure 1].

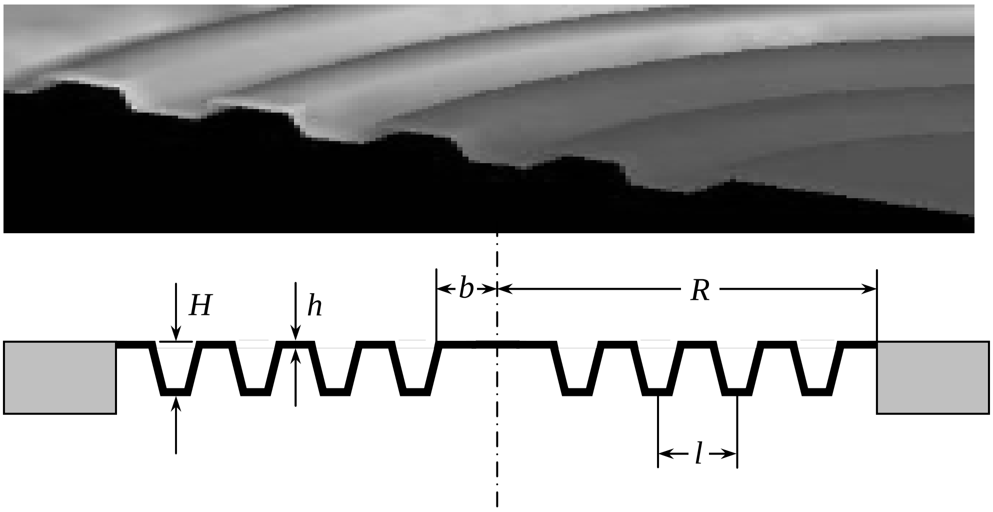

Figure (1) The schematic cross-sectional view of a circular corrugated diaphragm and design parameters (*R*: diaphragm radius, *b*: boss radius, *H*: corrugation depth, *h*: diaphragm thickness, *l*: corrugation pitch).

For shallow, sinusoidal corrugations the deflection is approximately given by [13]:

$$\frac{PR^4}{E'h^4} = A_p \frac{y}{h} + B_p \frac{y^3}{h^3}$$

where

$$A_p = \frac{2(q+3)(q+1)}{3\left(1-\frac{\nu^2}{q^2}\right)}$$

$$B_p = \frac{165(q+1)^3(q+3)}{q^2(q+4)(q+11)(2q+1)(3q+5)}$$

and

$$E' = \frac{E}{1-\nu^2}$$

and for shallow, sinusoidal profiles:

$$q^2 = 1 + 1.5\frac{H^2}{h^2}$$

with q the corrugation quality factor and H the corrugation depth. Thus q varies from 1, for a flat diaphragm, to a value that approaches 1.22 times the ratio of corrugation depth to diaphragm thickness. For conventional metal corrugated diaphragms, the value of q is typically chosen to be between 10 and 30. It is clear that the coefficient A_p increases rapidly with increases in q while the coefficient B_p decreases rapidly with increases in q. Thus the linearity of the diaphragm can be increased dramatically by providing corrugations that are as little as 3 times the diaphragm thickness. In this case, q=3.8, and the linear term, A_p is increased by about a factor of 4 while the cubic coefficient, B_p, is reduced by a factor of over 10.
In many useful structures it is desirable to introduce a center boss into the structure. This makes the structure more stiff for a given diaphragm thickness and corrugation depth. Small deflections of a bossed, corrugated diaphragm can be expressed as:

$$\frac{PR^2}{E'h^2} = A_p n_p \frac{y}{h}$$

where

$$\frac{1}{n_p} = \left(1-r^4\right)\left(1 - \frac{8qr^4\left(1-r^{q-1}\right)\left(1-r^{q-3}\right)}{(q-1)(q-3)\left(1-r^{2q}\right)}\right)$$

and r is the ratio of boss radius to diaphragm radius (*b/R*). This correction is less than 20% for boss ratios less than 0.4 with values of q greater than 4. It is very significant, however, for nearly flat diaphragms with boss ratios greater than 0.3. The influence of a boss on the cubic term is somewhat more complicated; a factor similar in magnitude to n_p can be used to modify the B_p term. A recent, quite extensive analysis is available in the work of Liu Renhuai [14].

FEA Simulation

The commercial finite-element code, ANSYS 9.0, is used for the simulations. The 3D models are created for both flat and corrugated diaphragms. In order to reduce the computation time, a quarter symmetric modeling technique is employed (figure 2). For solving the governing differential equation, FE model for the flat diaphragm is meshed with brick elements and the tetrahedral elements (free meshing) are taken for the corrugated diaphragm because of its complex geometry. Isotropic material properties were used for all the models. This can be justified for the silicon substrate because Chen et. al. [15] performed FEM on silicon using both isotropic 2-dimensional and anisotropic 3-dimensional modeling and found stresses within 3%. Chen et. al. [15] concluded that isotropic material properties are a good approximation for modeling silicon. Elastic properties are isotropic for cubic crystal thin films in the (111) crystallographic plane [16].

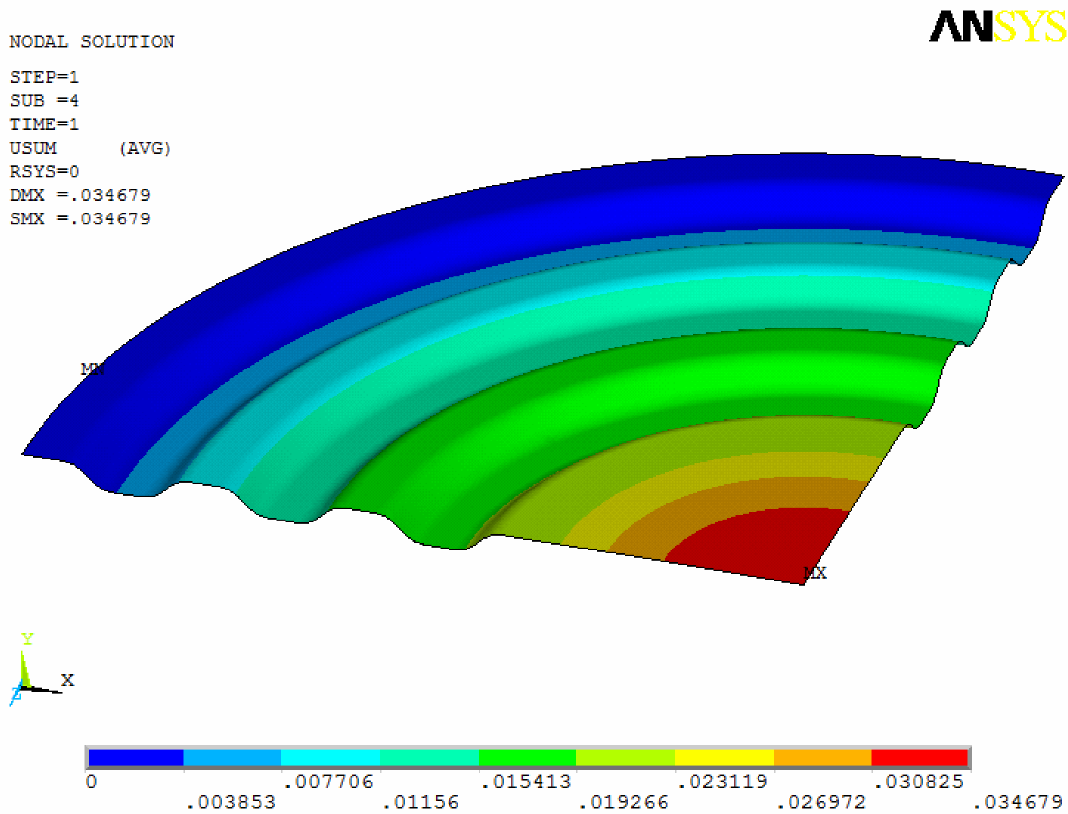

quarter symmetry model. Units are in mm.

Results and Discussions

The effects of design parameters on the load-deflection relation have been investigated using the above equations. The values of the independent design parameters used in this study are summarized in Table (2). Diaphragm diameter and thickness turned out to have high governing effect on load-deflection relation, as shown in figure 3. However, linear load-deflection relationship can be obtained by increasing corrugation depth. Therefore the rule of thumb in the design of a corrugated diaphragm is that increasing diaphragm diameter and/or decreasing diaphragm thickness increase diaphragm sensitivity and that increasing corrugation depth increases the linearity of load-deflection relation.

Table (2) Design parameters.

DESIGN PARAMETER	SYMBOL	VALUE
Diaphragm radius	R	1 ~ 5 mm
Diaphragm thickness	h	1 ~ 5 μm
Corrugation depth	H	10 ~ 35 μm
Boss ratio	r	0.1 ~ 0.8

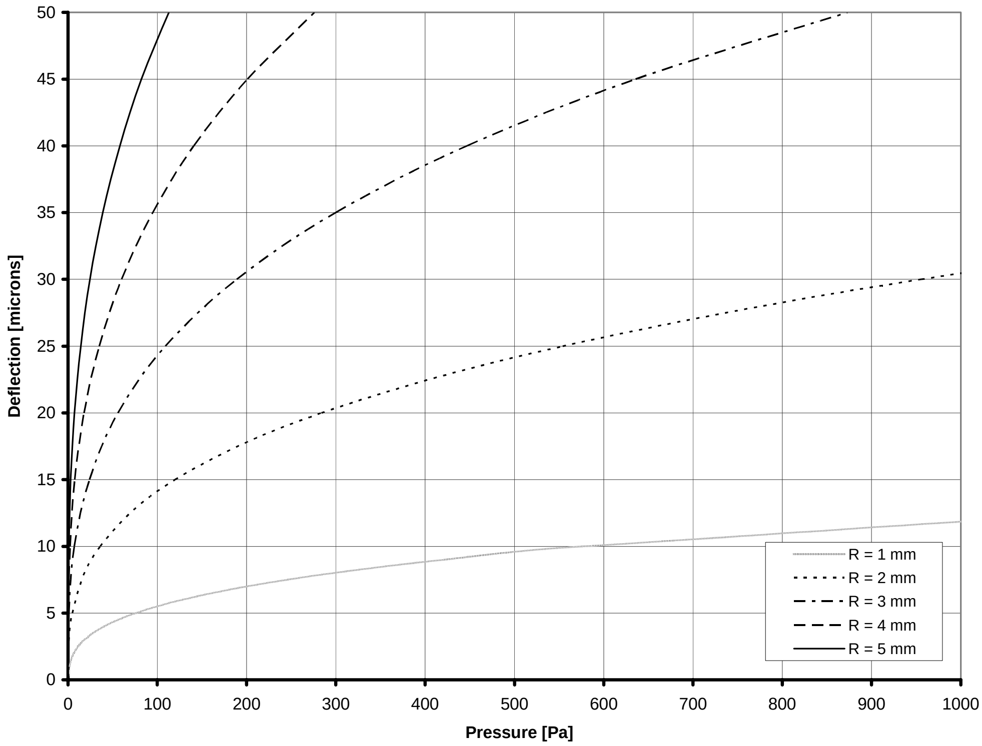

Figure (3 – a)

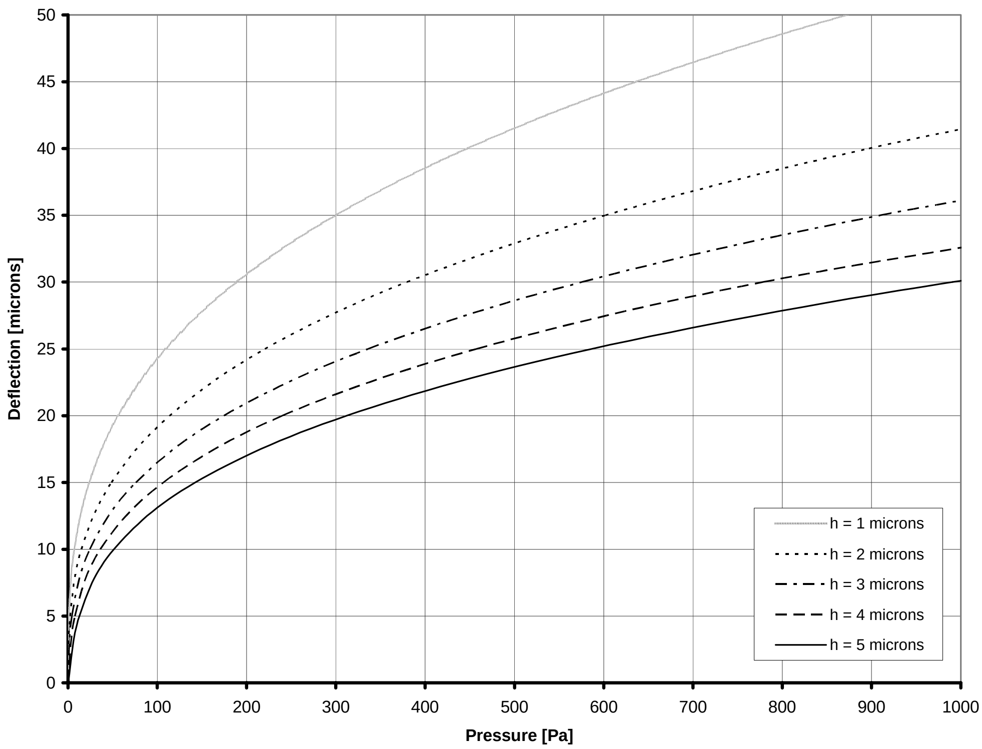

Figure (3 – b)

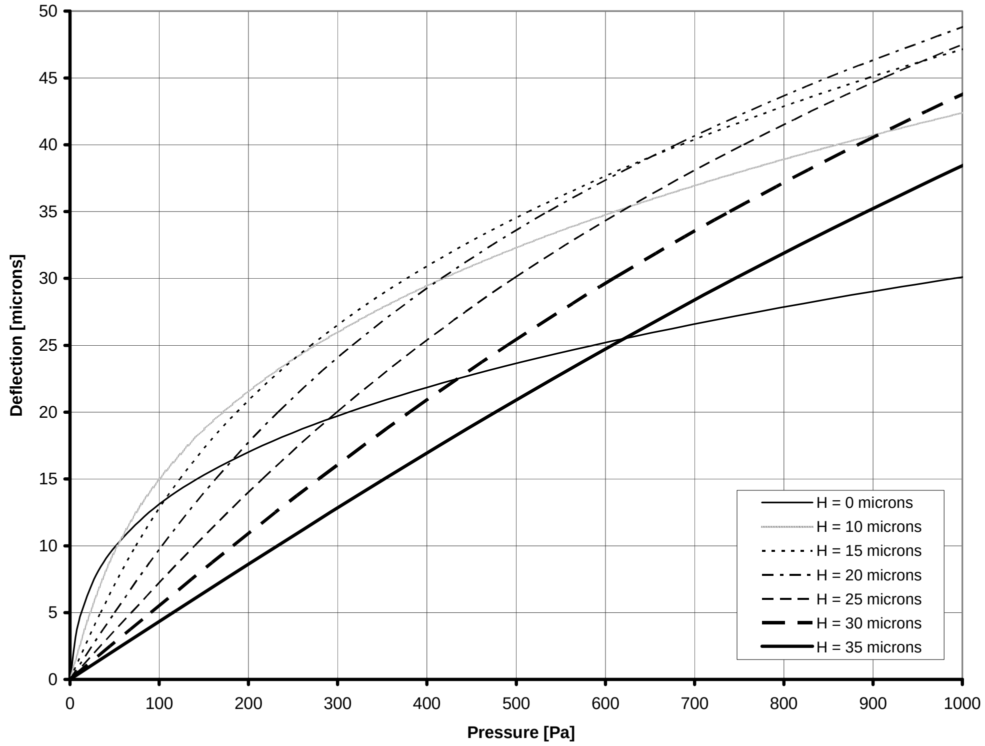

Figure (3 – c)

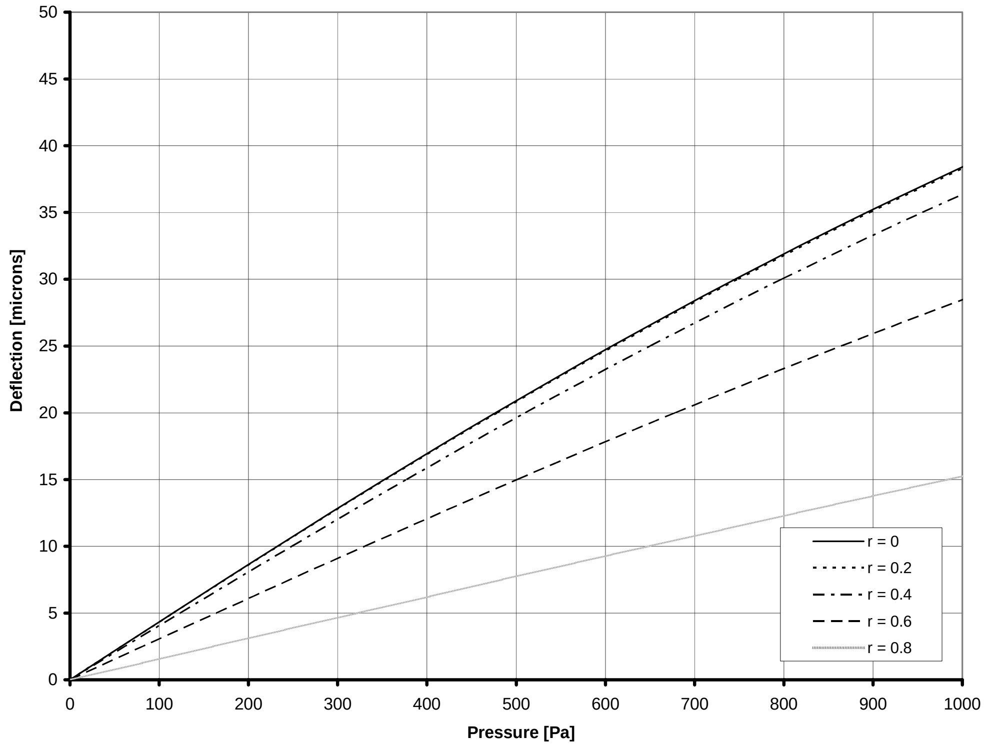

Figure (3 – d)

Figure (3) The effects of design parameters on the load-deflection relation:
(a) diaphragm radius, (b) diaphragm thickness, (c) corrugation depth, (d) boss ratio.

In the present work a number of different diaphragms have been simulated with a range of diameters, corrugation depths, diaphragm thicknesses, and boss ratios. Corrugation pitch did not show any noticeable effect compared to other parameters. A typical example is a 3 mm radius, circular diaphragm with a center boss radius of 1.2 mm (40%). The diaphragm thickness was 5 µm and the corrugation depth was 35 µm (figure 2). The deflection characteristics of these diaphragms with the theoretical results are shown in figure (4), for comparison.

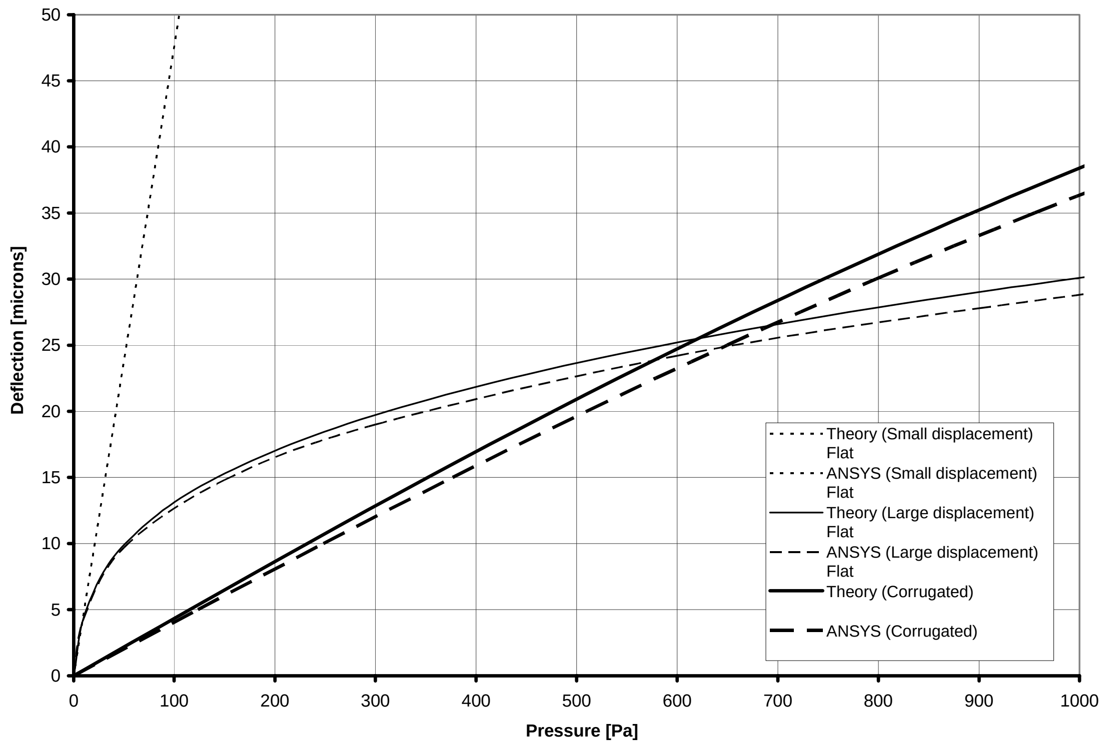

Figure (4) Comparison between theoretical and simulated results, R= 3 mm, h= 5 µm, H= 35 µm, and r= 0.4.

Conclusions

Using FEA with large displacement theory to simulate corrugated diaphragms is an effective method to get a good indication of the design parameters. In particular, applications requiring large, linear displacement are now possible by using corrugated shapes. These corrugations are introduced using processing techniques which are compatible with most other silicon processing techniques, not through the use of incompatible materials. Thus they should be useful in a wide variety of practical devices. The design information available from decades of work with corrugated metallic diaphragms appears applicable for use in silicon designs, again facilitating the use of these corrugated structures in practical devices.

References

[1] Shimazo, M., et. al., *A Silicon Diaphragm Pressure Sensor for Very Low Pressures*, Proceedings 3rd Sensor Symposium, Japan, 1983, p. 309.

[2] Suminto, J.T., et. al., *Silicon Diaphragm Capacitive Sensor for Pressure, Flow, Acceleration, and Attitude Measurements*, Proceedings Fourth International Conference on Solid-State Sensors and Actuators, Japan, 1987, p. 336.

[3] Jerman, J. H. and Mallinson, S.R., *A Miniature Fabry-Perot Interferometer Fabricated Using Silicon Micromachining Techniques*, Proceedings 1988 IEEE Solid-State Sensors and Actuators Workshop, p. 16.

[4] Wildhack, W.A. and Goerke, V.H., *Corrugated Metal Diaphragms for Aircraft Pressure-Measuring Instruments*, National Advisory Committee for Aeronautics, Technical Note 738, 1939.

[5] Mallon, J.R. and Kurtz, A.D., *Transducer Apparatus Employing Convoluted Semiconductor Diaphragms*, U.S. Patent #4,467,656, 1984.

[6] Stephen Beeby, et. al., *MEMS Mechanical Sensors*, London: Artech House, Inc., 2004.

[7] Judy, J. W., "Microelectromechanical Systems (MEMS): Fabrication, Design and Applications," *Smart Materials and Structures*, Vol. 10, 2001, pp. 1115–1134.

[8] Beeby, S. P., J. N. Ross, and N. M. White, *Design and Fabrication of a Micromachined Silicon Accelerometer with Thick-Film Printed PZT Sensors*, J. Micromech. Microeng., Vol. 10, No. 3, 2000, pp. 322–329.

[9] Beeby, S. P., M. Stuttle, and N. M. White, *Design and Fabrication of a Low-Cost Microengineered Silicon Pressure Sensor with Linearized Output*, IEE Proc. Sci. Meas. Technol., Vol. 147, No. 3, 2000, pp. 127– 30.

[10] Cook, J., *Fundamentals of Sensor Technology: Pressure*, Proc. Sensors Expo., Baltimore, MD, May 4–6, 1999, pp. 401–415.

[11] Di Giovanni, M., *Flat and Corrugated Diaphragm Design Handbook*, New York: Marcel Dekker, 1982.

[11] Bert, C. W. and Martindale, J. L., *An Accurate, Simplified Method for Analyzing Thin Plates Undergoing Large Deflections*, J. AIAA, vol. 26, n. 2, Feb. 1988, p. 235.

[12] Hin-Leung Chau and Wise, K. D., *Scaling Limits in Batch Fabricated Silicon Pressure Sensors*, IEEE Trans. Elec. Dev., vol. ED-34, n. 4, April 1987, p. 851.

[13] Haringx, J. A., *Design of Corrugated Diaphragms*, ASME Transactions, vol. 79, 1957, p. 55.

[14] Liu Renhuai, *Nonlinear Analysis of Corrugated Annular Plates Under Compound Load*, Scientia Sinica, Ser. A, vol. 27, n. 9, Sept. 1985, p. 959.

[15] K. Chen, A. Ayon, and S. Spearing, *Controlling and Testing the Fracture Strength of Silicon on the Mesoscale*, Journal of the American Ceramic Society, Vol. 83, No. 6, pp. 1476-84, 2000.

[16] J. Mitchel, *Characterization of Mechanical Properties of Cubic Silicon Carbide Thin Films Deposited Onto Silicon*, M.Sc. Thesis, Case Western Reserve University, Cleveland, OH, 2000.